Electronic Supplementary Material (ESI) for Biomaterials Science.

Supplementary information

Yield by weight	58%
Molecular weight (g/mol ± % 0.95 CI)	1.841×10^4 (± 6.2335%)
Polydispersity index (± % 0.95 CI)	1.637 (± 8.815%)
EGDPEA conversion	57%
DEGMA conversion	>99%
Feed monomer ratio	1.3:1

Table S1 | GPC and ^{1}H NMR results for EGDPEA:DEGMA. Yield by weight, molecular weight, polydispersity index, monomer ratios and feed monomer ratios of synthesised EGDPEA:DEGMA, ascertained by GPC and ^{1}H NMR analysis. The ± percentage values for molecular weight and polydispersity index are 0.95 confidence interval variances.

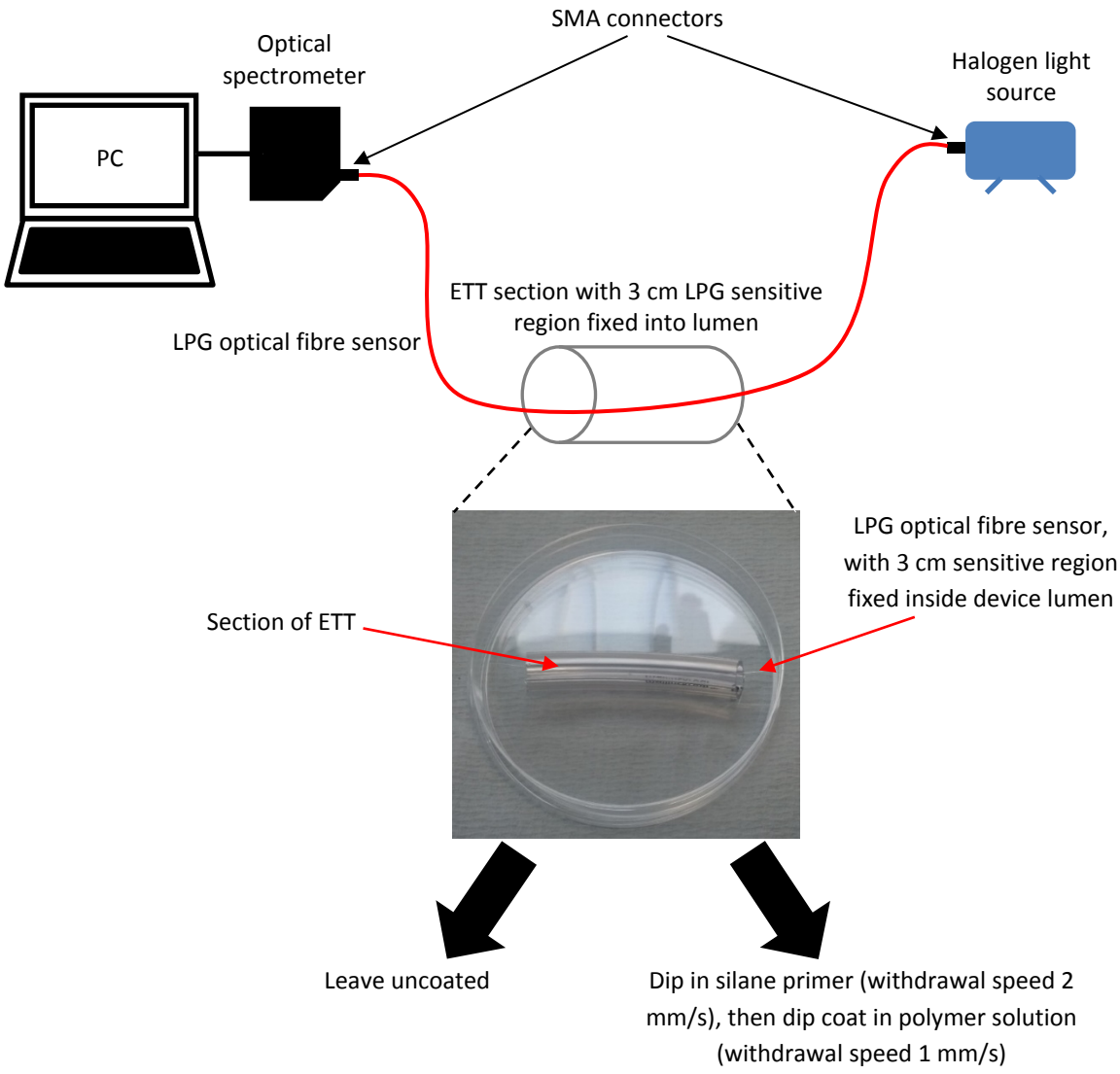

Figure S1| Set up of LPG optical fibre instrumented ETT. Experimental set up of LPG sensor in ETT lumen, showing the halogen light source, SMA connectors and optical spectrometer. The 3 cm sensitive region of the optical fibre is inside the device lumen, in contact with the inner wall. The combined sensor-ETT system was either left uncoated or dip coated in the silane adhesion promoter (primer) and then EGDPEA:DEGMA solution.

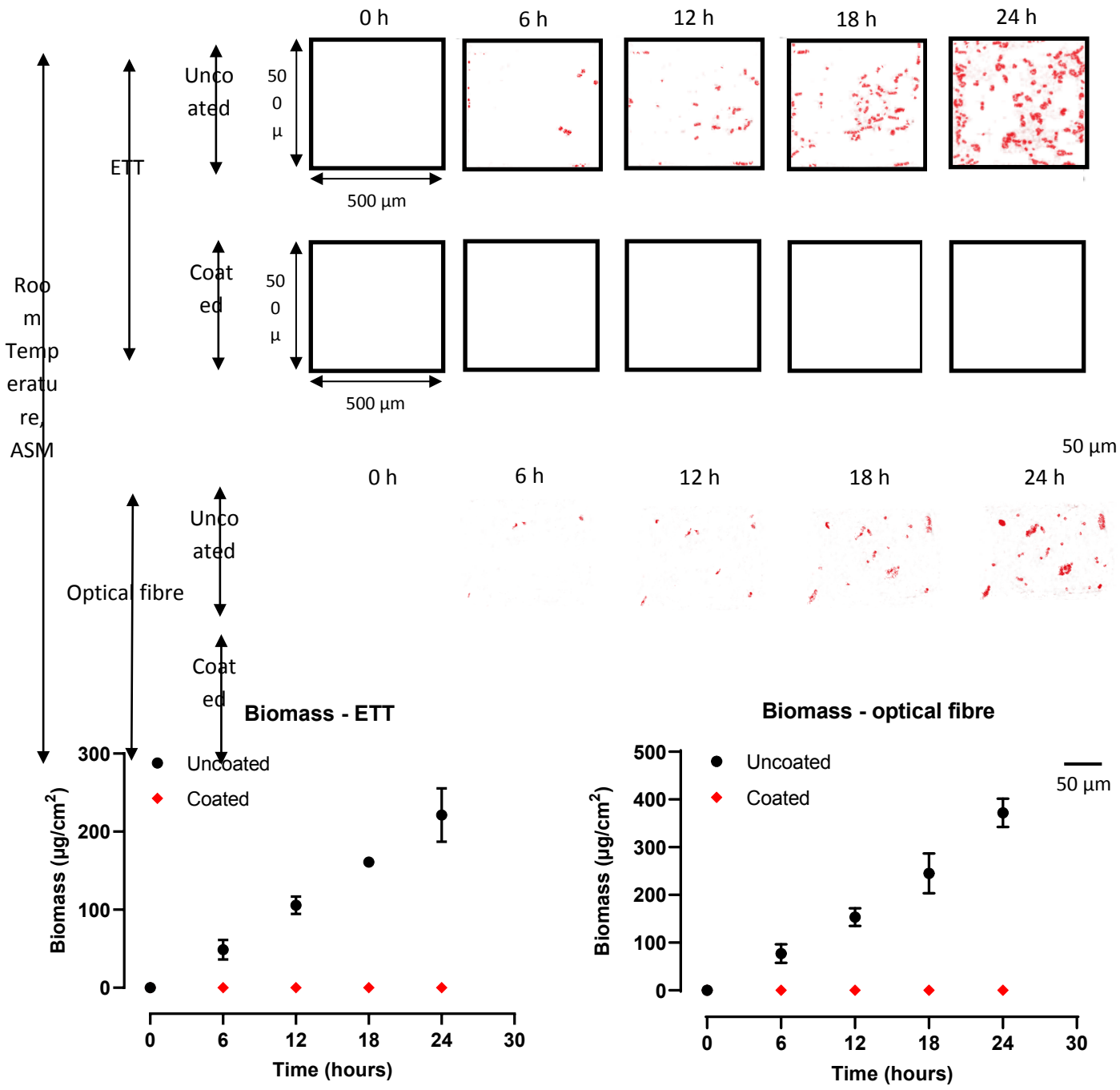

Figure S2 | Confocal microscopy quantification of *P. aeruginosa* biofilms in ETTs and on optical fibres in ASM at room temperature. 2D and 3D confocal images of *P. aeruginosa* biofilms on uncoated and coated ETTs and optical fibres respectively, at 6 h intervals for 24 h, at room temperature, in ASM. The red areas represent biofilm, as the *P. aeruginosa* was transformed to express fluorescent mCherry (excitation = 587 nm, emission = 610 nm). All ETT images are 500 x 500 µm and the scale bar for all optical fibre images is 50 µm. Quantification of biomass for both samples, using COMSTAT, with a fluorescence threshold of 56 AU. Measurements are mean biomass ± s.d, N = 3.

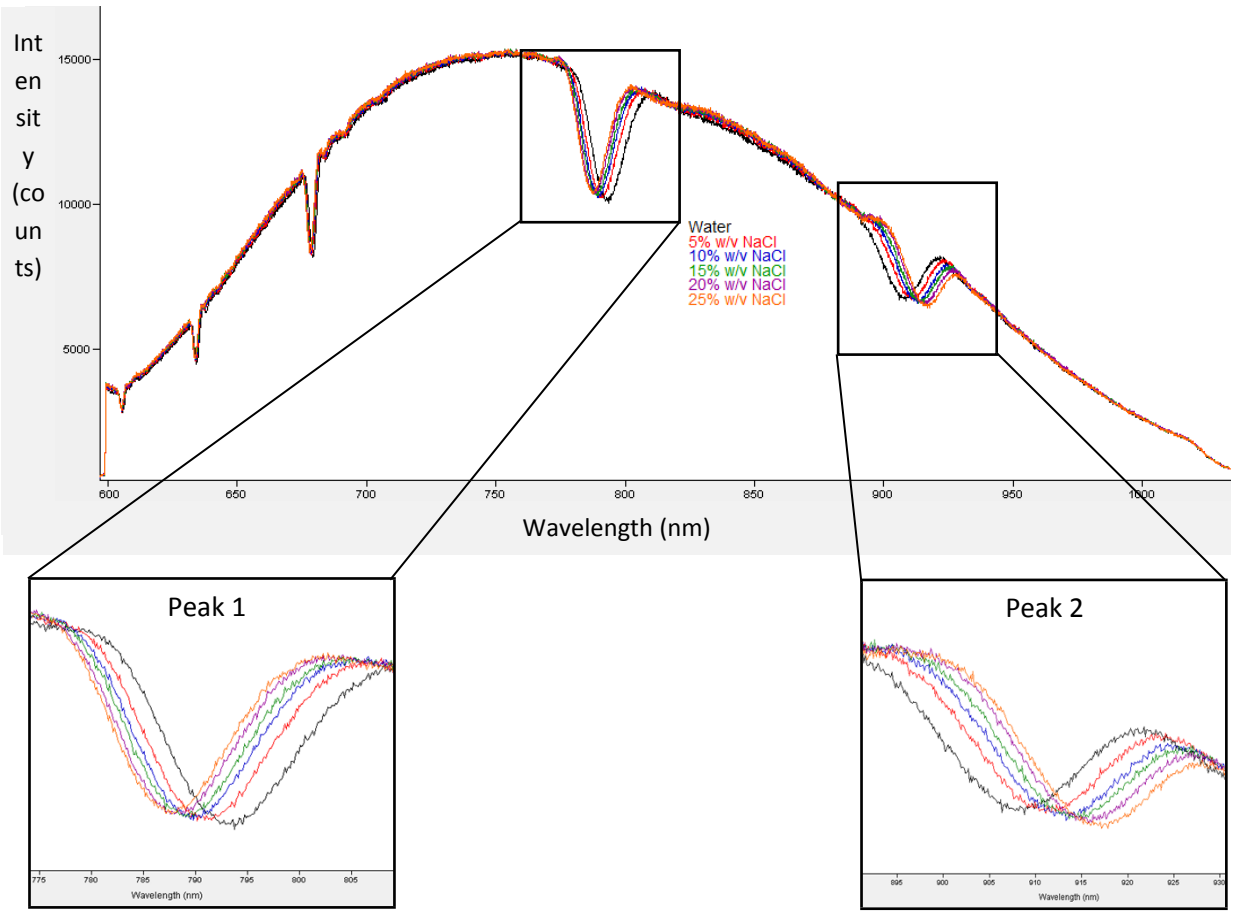

Figure S3 | Calibration of uncoated LPG sensor. Transmission spectra from uncoated LPG sensor exposed to sodium chloride solutions of increasing concentration, presented in SpectraSuite. Peaks 1 and 2 are enlarged.

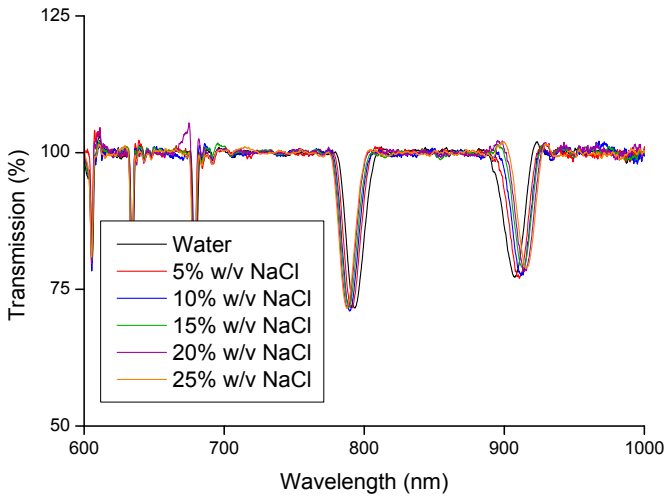

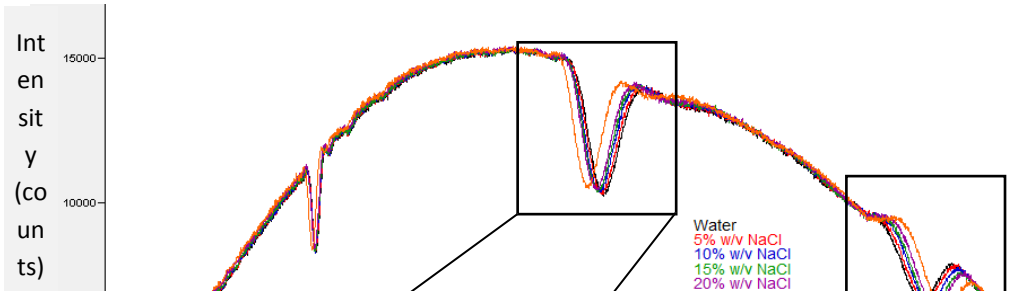

Figure S4 | Processed transmission spectra. Processed spectra, using OriginPro 8.6, for the calibration of uncoated LPG optical fibre sensors in sodium chloride solutions. Note the change in the *y*-axis from intensity to transmission percentage.

Figure S5 | Calibration of coated LPG sensor. Transmission spectra from coated sensor exposed to sodium chloride solutions of increasing concentration, presented in SpectraSuite. Peaks 1 and 2 are enlarged.

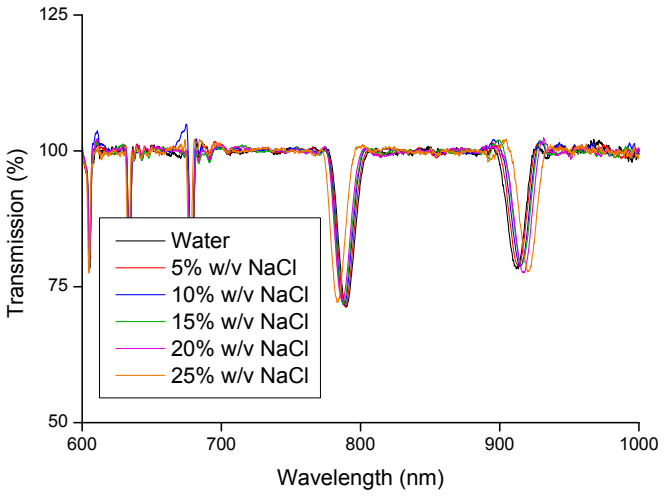

Figure S6 | Processed transmission spectra. Processed spectra, using OriginPro 8.6, for the calibration of coated LPG optical fibre sensors in sodium chloride solutions. Note the change in the *y*-axis from intensity to transmission percentage.

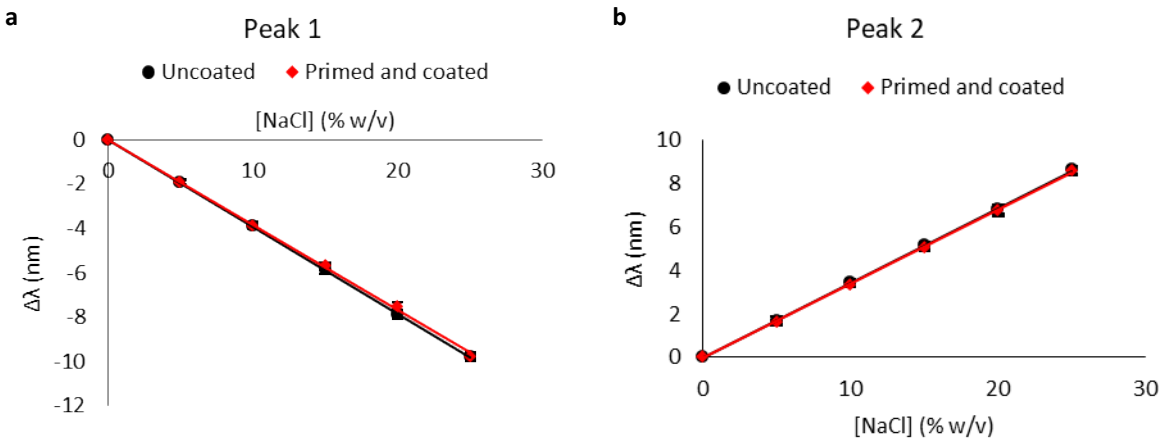

Figure S7 | Wavelength shift for sodium chloride calibration. a, Peak 1 wavelength shift and **b,** Peak 2 wavelength shift, for uncoated and coated LPG sensors with increasing sodium chloride concentration (Figures. S3-S6). Error bars are ± s.d, n = 3.

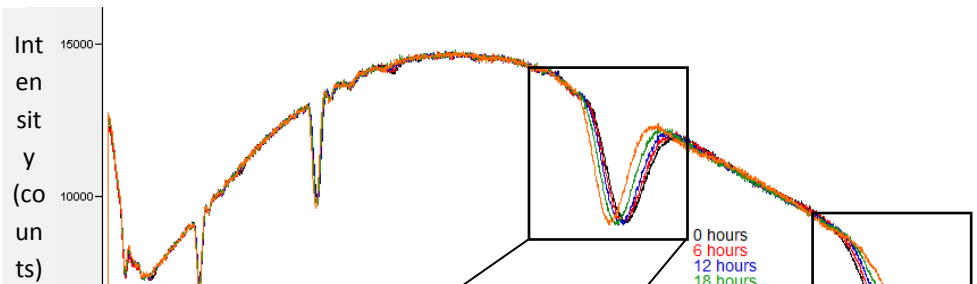

Figure S8 | Transmission spectra from exposure of sensor-ETT system to *P. aeruginosa* ASM culture medium. Transmission spectra from the uncoated LPG sensor-ETT system exposed to *P. aeruginosa* cultured in ASM. Spectra are displayed in SpectraSuite, at 6 h intervals for 24 h. Peaks 1 and 2 are enlarged.

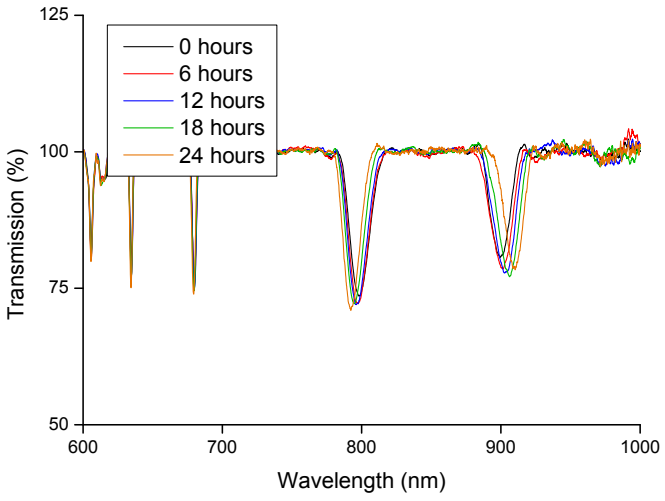

Figure S9 | Processed transmission spectra. Processed spectra, using OriginPro 8.6, for the exposure of uncoated sensor-ETT systems to *P. aeruginosa* culture, in ASM. Note the change in the *y*-axis from intensity to transmission percentage. No wavelength shift was observed for the coated system.

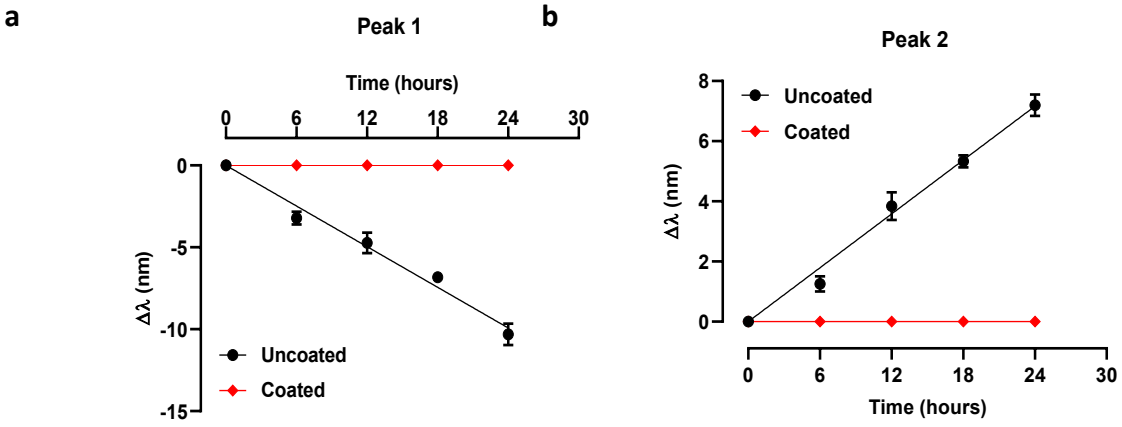

Figure S10 | Wavelength shifts in RPMI-1640 medium. a, Wavelength shift (Δλ) of peak 1 from uncoated and coated LPG sensor-ETT systems immersed in *P. aeruginosa* RPMI-1640 cultures for 24 h. Error bars are ± s.d, N = 3. **b,** Wavelength shift (Δλ) of peak 2 from uncoated and coated LPG sensor-ETT systems immersed in *P. aeruginosa* RPMI-1640 cultures for 24 h. Error bars are ± s.d, N = 3.

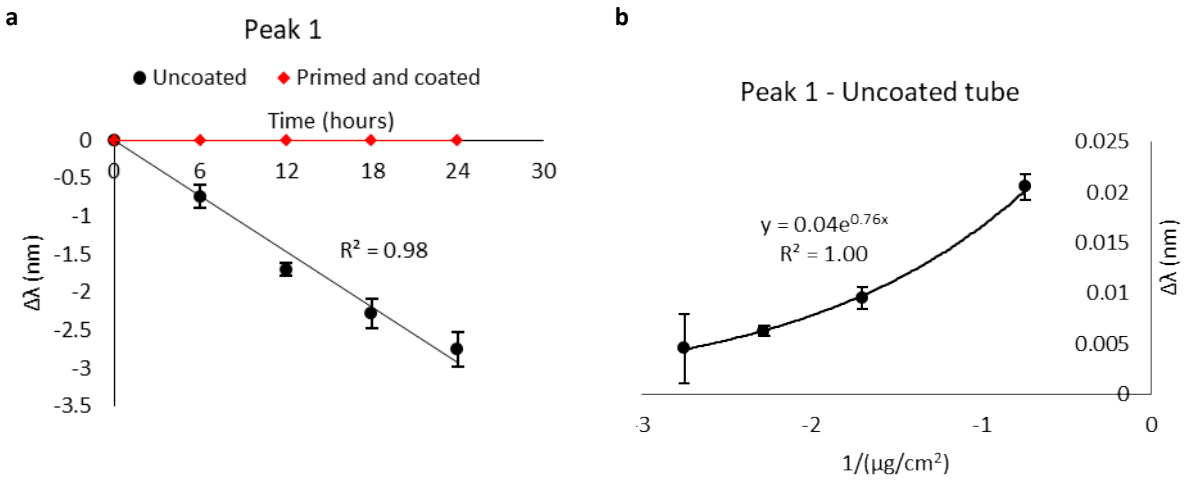

Figure S11 | Response from LPG sensor instrumented ETT. a, Wavelength shift (Δλ) of peak 1 from uncoated and coated LPG sensor-ETT systems immersed in *P. aeruginosa* cultures in ASM for 24 h, at room temperature. Error bars are ± s.d, N = 3. **b,** Plot of peak 1 wavelength shift from **a** against the inverse biomass of *P. aeruginosa* biofilms grown on uncoated ETT sections in ASM. An exponential function is fitted to the data. Error bars are ± s.d of biomass, N = 3.

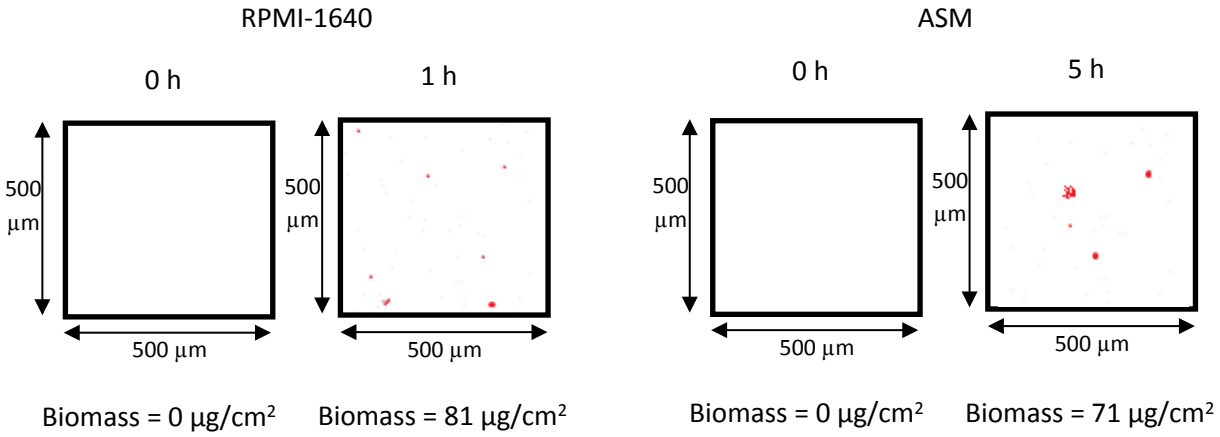

Figure S12 | 2D CLSM images and quantified biomass for sensitivity calculation. 2D CLSM images of *P. aeruginosa* biofilms grown on uncoated ETT sections, in RPMI-1640 medium (left) and ASM (right), at 0 and 1 h (RPMI-1640) and 0 and 5 h (ASM), when a measurable wavelength shift occurred. Biofilm is represented by the red areas. Images are 500 µm x 500 µm. The biomass was quantified in COMSTAT at each time point and is labelled below the images, obtained using a COMSTAT fluorescent threshold of 56 AU.

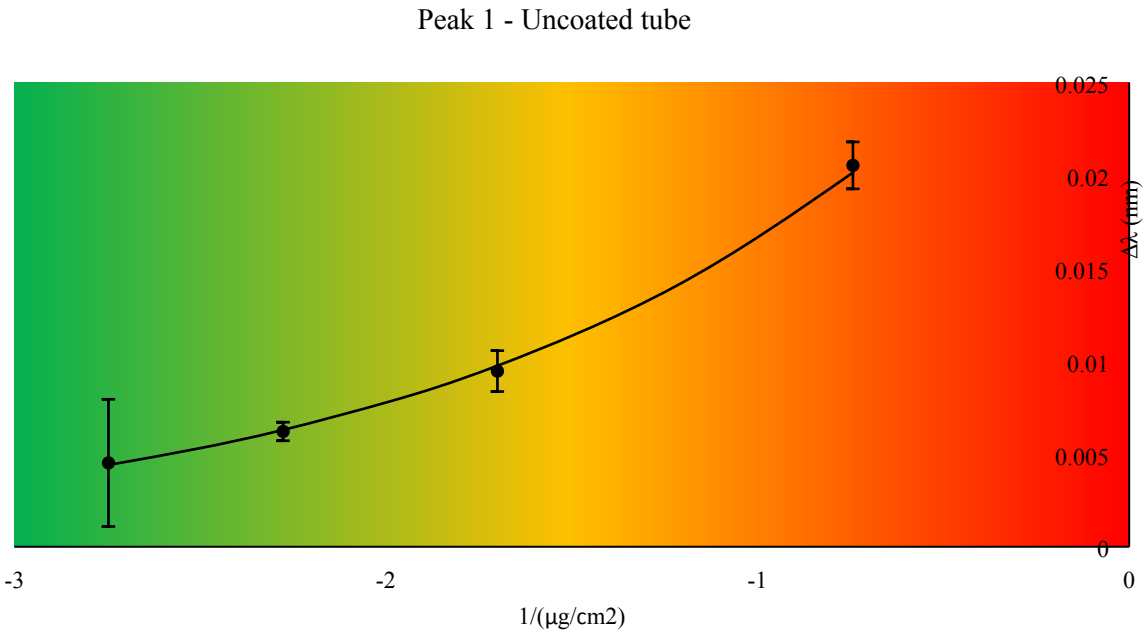

Figure S13 | Traffic light system for infection prediction. Exponential relationship between peak 1 wavelength shift and inverse biomass for the uncoated LPG sensor-ETT system, exposed to *P. aeruginosa* grown in ASM for 24 h. Error bars are ± s.d of biomass, N = 3. A traffic light colour scheme indicates the 'safety' of the device, predicted by the wavelength shift only (green = safe, red = unsafe).

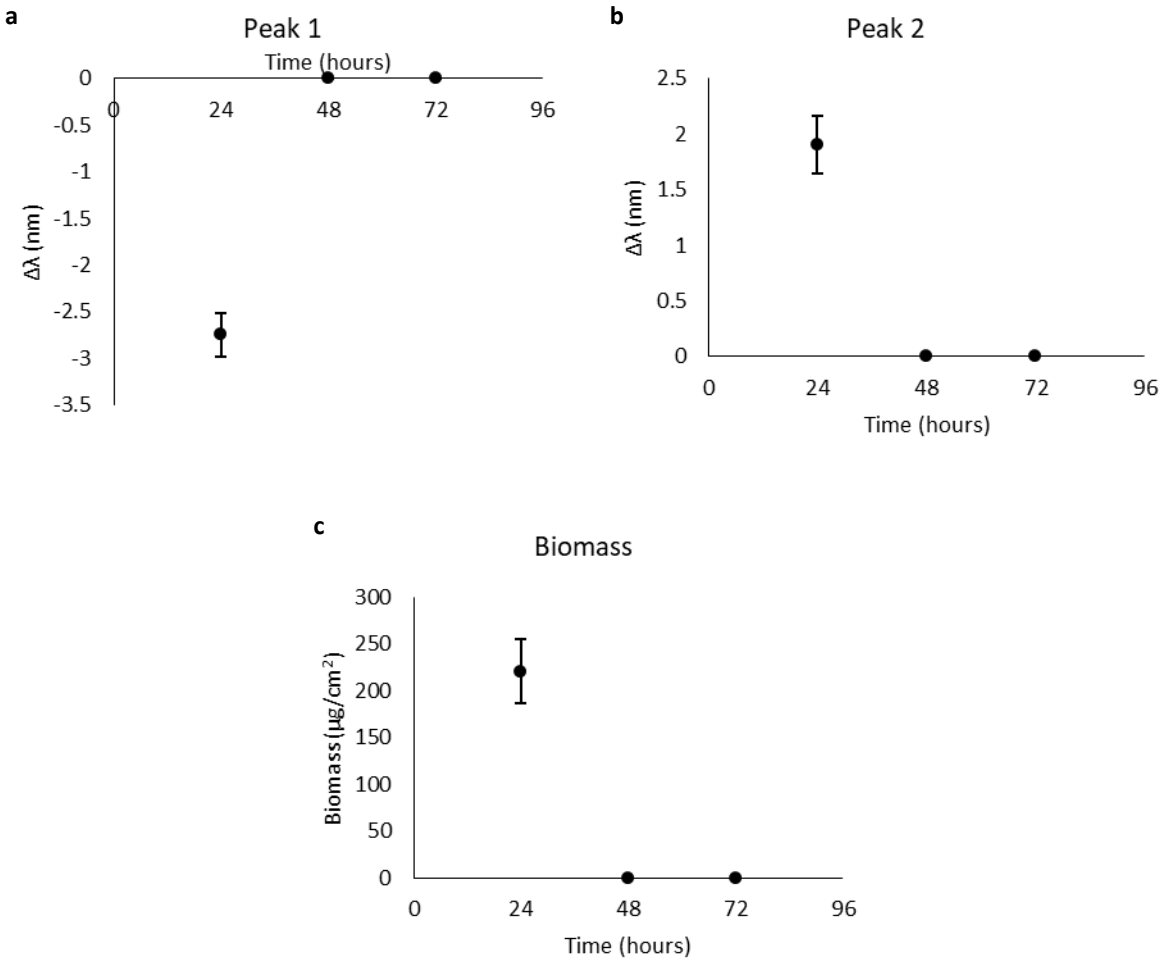

Figure S14 | Wavelength shift and biomass decrease upon biofilm disintegration. a, Peak 1 wavelength shift from uncoated LPG sensor-ETT systems exposed to *P. aeruginosa* in ASM at 24, 48 and 72 h. Error bars are ± s.d, N = 3. **b,** Peak 2 wavelength shift from uncoated LPG sensor-ETT systems exposed to *P. aeruginosa* in ASM at 24, 48 and 72 h. Error bars are ± s.d, N = 3. **c,** Quantified biomass from CLSM images of *P. aeruginosa* on ETT sections in ASM at 24, 48 and 72 h, obtained at a COMSTAT fluorescence threshold of 56 AU. Error bars are ± s.d, N = 3.

The above demonstrates the ability of the LPG optical fibre sensor to detect biofilm disintegration. As biomass fell between 24 and 48 h, both peaks' wavelength shift returned to zero, indicating a decrease in refractive index at the sensor surface, as the biofilm (adsorbed cells and EPS) fell away from the surface. We therefore propose that the sensor could be used to monitor biofilm dispersal or death (and the patient's infection 'status') during for example, antibiotic treatment.

Artificial Sputum Medium Composition

Taken from Palmer *et al*. (2007)[51].

Synthetic Cystic Fibrosis Sputum Medium (SCFM) was developed from the average concentrations of ions, free amino acids, glucose, and lactate in cystic fibrosis (CF) sputum samples. For amino acids, the percentage of total free amino acids in each CF sputum sample was determined for individual amino acids. The average percentage of each amino acid was extrapolated to a final total amino acid concentration of 19 mM for SCFM. Amino acids were maintained as 100 mM stocks in deionized water and stored in the dark at 4°C. Tyrosine, aspartate, and tryptophan were resuspended in 1.0 M, 0.5 M, and 0.2 M NaOH, respectively. Lactate stocks were adjusted to a pH of 7.0 with NaOH.

For SCFM, amino acids were added from 100 mM stocks to a buffered base (6.5 mL 0.2 M NaH_2PO_4, 6.25 mL 0.2 M Na_2HPO_4, 0.348 mL 1 M KNO_3, 0.122 g NH_4Cl, 1.114 g KCl, 3.03 g NaCl, 10 mM MOPS, 779.6 mL deionized water) in the following volumes: L-aspartate, 8.27 mL; L-threonine, 10.72 mL; L-serine, 14.46 mL; L-glutamate·HCl, 15.49 mL; L-proline, 16.61 mL; L-glycine, 12.03 mL; L-alanine, 17.8 mL; L-cysteine·HCl, 1.6 mL; L-valine, 11.17 mL; L-methionine, 6.33 mL; L-isoleucine, 11.2 mL; L-leucine, 16.09 mL; L-tyrosine, 8.02 mL; L-phenylalanine, 5.3 mL; L-ornithine·HCl, 6.76 mL; L-lysine·HCl, 21.28 mL; L-histidine·HCl, 5.19 mL; L-tryptophan, 0.13 mL; and L-arginine·HCl, 3.06 mL. SCFM was adjusted to pH 6.8 and filter sterilized through a 0.2-µm-pore-size filter. After sterilization, the following sterile components were added per litre: 1.754 mL 1 M $CaCl_2$, 0.606 mL 1 M $MgCl_2$, and 1 mL 3.6 mM $FeSO_4 \cdot 7H_2O$.

LPG optical fibre sensor considerations

LPG optical fibre sensors have a glass core of higher refractive index than the glass cladding, causing input light to be totally internally reflected[53]. Modulating the refractive index of the core using UV laser irradiation leads to gratings, allowing the core mode to couple into certain cladding modes, resulting in attenuation bands (losses of transmission) centred at discrete wavelengths[34-36]. Changes to the refractive index near the cladding causes a change in the optical properties of the cladding (cladding mode effective refractive index), in turn causing a shift in the wavelength of attenuation bands[27,28]. This shift can be measured, allowing the LPG optical fibre to be used for sensing.

In all the experiments conducted in this study, two attenuation bands (or peaks) were present in the optical/transmission spectra (for example, Figure 4). This was caused by core-cladding mode coupling occurring at two different wavelengths, referred to as dual resonance[38]. This phenomenon occurs with coupling at or near the phase-matching turning point (PMTP), which exists in the phase matching condition[38,39]. Typically, coupling at the PMTP results in a single broad attenuation in the optical spectrum, which splits as external refractive index increases[39]. Further increases in refractive index cause the peaks to continue separating, causing the opposing shifts of peaks, as seen, for example, in Figure 4, or in the calibration (Figure S7). Increases in media refractive index changed the cladding effective index, causing core-cladding mode coupling at 'wider' wavelengths[38,39]. This is the fundamental property of LPG optical

fibre sensors; their ability to sense changes in refractive index makes them attractive for a wide range of sensing applications. LPG optical fibre sensors with gratings allowing for coupling near or at the PMTP have the highest sensitivity to refractive index[36-38].

The purpose of the calibration was to ensure that the sensor could detect changes in medium refractive index and to compare uncoated with coated LPG optical fibre sensor responses. Figure S7 shows linear increases in wavelength shift with increasing sodium chloride concentrations. Increasing solute concentrations also increased the refractive index of the solutions, in a step-wise manner. This in turn changed the cladding effective index step-wise[34-36], causing core-cladding mode coupling to occur at wavelengths shifted to the left and right of peaks 1 and 2 respectively. The shifts were linear, due to the linear (step-wise) changes in medium refractive index[34-36]. There were no differences in wavelength shift of either peak between uncoated and coated LPG optical fibre sensors.

The effective sensing distance from the cladding surface is determined by the evanescent field around the cladding[40,41], which decays exponentially with distance from the cladding surface[42]. The evanescent field size is dependent upon the grating period and the optical nature of the material deposited onto sensor surfaces[54]. The sensing 'radius' around the optical fibre has been reported to be between 50 and 800 nm[55,56]. The average coating thickness on the optical fibre surface was about 500 nm, hence the cladding modes propagated through the evanescent field further than 500 nm, since a response was observed for the coated LPG sensor in sodium chloride solutions. Furthermore, larger biofilms extending beyond the evanescent field range introduced a third waveguide, which essentially 'extends' the coupling range of core modes, allowing coupling beyond the cladding[63]. This likely allowed the LPG sensor to detect changes in refractive index (biofilm formation) beyond the perceived evanescent field.

Although the application of the primer and coating lead to a positional change of the attenuation bands in water (due to a deposited film of higher refractive index than air), there was no difference in the wavelength shift profiles between uncoated and coated LPG sensors (Figure S7). This suggests that the primer and coating did not dampen the sensitivity of the sensor, nor did they change core-cladding coupling behaviour. Coupling did occur at different wavelengths but the change in cladding mode effective index occurred at the same rate for both LPG sensor surface modifications. Therefore, differences in wavelength shifts in bacteria culture medium would be due to differing rates of cell attachment between uncoated and coated sensors.

Upon exposure of the sensors to *P. aeruginosa* growth in ASM, linear wavelength shifts occurred on the uncoated sensor. Again, this represents linear changes in refractive index (and subsequently linear increases to cladding mode effective index)[34-36]. As discussed, it therefore appears that the refractive index was increasing linearly. This was attributed to bacterial cell growth and EPS production over time, the latter of which was not imaged by confocal microscopy. This led to a linear wavelength shift change but a non-patterned biomass change (Figure 4), which ultimately resulted in the exponential relationship between wavelength shift and biomass. The coated sensor prevented biofilm formation; hence no refractive index change

was measured near the sensor surface, resulting in zero wavelength shift, which was corroborated by the zero biomass change shown in Figures 2 and S2.